THE EFFECTS OF HUMIDITY AND GAS PHASE CONCENTRATION ON

THE ABSORPTION OF SULFUR DIOXIDE BY CHARGED AQUEOUS DROPLETS

Approved:

Michael J. Matteson, Chairman

Clyde Orr, Jr.

Henderson C. Ward

Date approved by Chairman: 3/2/73

THE EFFECTS OF HUMIDITY AND GAS PHASE CONCENTRATION ON THE ABSORPTION OF SULFUR DIOXIDE BY CHARGED AQUEOUS DROPLETS

A THESIS

Presented to

The Faculty of the Division of Graduate

Studies and Research

By

Philip Joseph Giardina

In Partial Fulfillment

of the Requirements for the Degree

Master of Science in Chemical Engineering

Georgia Institute of Technology

February, 1973

ACKNOWLEDGMENTS

I would like to express my gratitude to my thesis advisor, Dr. Michael J. Matteson, for his direction and encouragement. Also, my thanks go out to Mr. Edwin Hartley for his patience and generosity in sharing laboratory equipment. Finally, I would like to express my appreciation to the Department of Health, Education and Welfare for its financial support during this research.

TABLE OF CONTENTS

LIST OF TABLES

LIST OF ILLUSTRATIONS

SUMMARY

Work by other investigators has indicated that the rate of absorption of sulfur dioxide by water droplets can be increased by applying electrical charges to the surface of the droplets. Also, it has been indicated that absorption takes place most rapidly during the time when the droplets are being formed, irrespective of the presence of applied surface charge. With this background in mind, this study was structured to examine the effect that applied surface charge would have on the absorption of sulfur dioxide by a growing water droplet. Specifically, the study was concerned with the effect of the ambient humidity and the effect of the concentration of sulfur dioxide in the reactant gas stream on the absorption rate. An adsorption theory was proposed whereby the number of sites on the droplet surface available for the adsorption of sulfur dioxide molecules was increased in direct proportion to the square of the surface charge density. Further, the rate of mass transfer was theorized to be linearly related to the reactant gas stream concentration. In measuring mass transfer rates, it was found that the data correlated well with the proposed theory and that, by applying a surface charge density of 6 statcoulombs/cm^2, the rate of mass transfer could be increased by roughly 60%. Ambient humidity was found to have no effect on this phenomenon.

CHAPTER I

INTRODUCTION

Over the last ten years the United States has developed a deep national conscience regarding the growing and serious problem of air pollution. Awareness of this problem and the committment to end all forms of atmospheric contamination are evidenced by the establishment of presidential councils and agencies for the purpose of establishing and maintaining appropriate limits on all emissions to the air. As another example, the possibility of adverse effects on the atmosphere was an important factor leading to the cancellation of the SST program by Congress. Each year greater and greater amounts of pollutants such as soot particles, oxides of nitrogen, carbon monoxide, and sulfur dioxide are pumped into our atmosphere. Although much effort and money are being channelled to end this pollution, the problem continues to grow.

One of the more significant parts of this problem is the reduction of sulfur dioxide emissions to the atmosphere. As the nation expands its demand for electrical energy, more and more fossil-fueled power plants are required to meet the demand. Since these power plants are the prime producers of sulfur dioxide, some effective means of removing this pollutant from power plant stack gases is required. Methods currently employed leave something to be desired either in economics or in efficiency.

In most of the anti-pollution systems currently in use, some form of wet scrubbing is usually employed. In this scrubbing, a liquid, usually water, is brought into contact with the stack gas and the sulfur dioxide is absorbed by the liquid. One approach to increasing the removal of sulfur dioxide from stack gases would be to improve the efficiency of wet scrubbing, i.e., increase the amount of pollutant absorbed per unit of liquid. To develop a method that would accomplish this increased absorption, it is important to study the mechanisms and phenomena that are occurring during the absorption. Such a study poses some difficulty, though, as may be seen in this quotation from Bird, et al. (5) in their book Transport Phenomena.

> Two-fluid mass-transfer systems offer many challenging problems: the flow behavior is complicated, the moving interface is virtually inaccessible to sampling, the interfacial area is usually unknown, and many of the practically important systems involve liquid phase chemical reactions. A better basic understanding of these systems is needed.

Earlier investigators have studied the effects of various physical parameters on the absorption of a gas by a liquid. These parameters include the composition of the phases, the temperature of the phases, contact times, and the solubility of the phases. However, little work has been done to examine the effect of surface electrical charge on gas-liquid absorption. Some study has occurred on the effect of electric fields on condensation. The famous Wilson cloud chamber experiment is based on the fact that ions assist in the nucleation of super-saturated water vapor. Unfortunately, this phenomenon has not yet been suitably explained on a theoretical basis. At the 1971 National Meeting of

the American Institute of Chemical Engineers, Mr. A. M. Marks (17) of the Marks Polarized Corporation presented a paper entitled "Charged Aerosols for Air Purification and Other Uses." He described a device that could absorb noxious gases efficiently if it could operate at a temperature below 100°C. The device was a venturi scrubber with the aqueous solution introduced through a metal capillary maintained at a high electric potential. This field produced a very fine aerosol in the venturi throat. The large surface area of the aerosol permitted excellent absorption efficiencies. There was not, though, any measurement of the aerosol size or the amount of aerosol entrained by the gas flow. Thus, there was no method of quantifying the effect of the electric field on the gas absorption. At least Marks had shown that, in general, charged aerosols can be used to increase significantly the absorption rates of certain noxious substances. Further investigation of this phenomena was, therefore, warranted.

Davis (9) performed an experiment in which he formed charged droplets at the tip of a capillary, then allowed the droplets to fall countercurrently through a rising gas stream. He examined the absorption at two humidities, 35% and 90%, and at only one concentration, 2000 parts per million of sulfur dioxide in air. Though speculating on the possible effects of gas phase concentration and relative humidity, his main purpose was to demonstrate that application of surface electrical charge would significantly enhance the absorption of sulfur dioxide by water droplets. His work lent more weight to the phenomenon that Marks had displayed.

In searching the literature, it was found that the subject of mass

transfer into droplets has been studied for a number of years, with theories having been postulated as early as the 1930's. Regretfully, though, this work was done primarily in the area of liquid-liquid extraction. Though not exactly the same in nature as this study, these efforts have produced some worthwhile information. Higbie (13) noted that steady flow conditions, which had been assumed in earlier theoretical developments, are never reached in ordinary types of industrial equipment. Licht and Conway (15) identified three separate stages in droplet mass transfer: the drop formation time, the time of rise (or fall) through the continuous medium, and the drop coalescence period at the terminal end of the reactor. They noted further that the rate of absorption was greatest in the drop formation stage, and that during this stage the solute is not transferred by the ordinary process of diffusion. Finally, Angelo (2) has reported mass transfer coefficients for the case of droplet formation periods that were fifteen times as great as those predicted by boundary layer calculations. Since droplet formation was apparently a significant period in the overall absorption process, this period was selected on which to superimpose the subject study of the effects of surface charge on gas-liquid absorption.

In this research, then, it was desired to verify that the presence of surface charge on water droplets would enhance sulfur dioxide absorption, to observe the effect of relative humidity, and to report the effect that different concentrations in the gas phase would have on the absorption process. All this was accomplished by applying a given surface charge density to water droplets which were continuously being formed at the tip of a charged capillary that was exposed to air con-

taining a known concentration of sulfur dioxide. As soon as the droplets fell from the capillary, contact with the sulfur dioxide-air stream ceased, and the droplets were collected for later analysis. This particular experimental design overcomes the problem of requiring a droplet to fall great lengths through a gas stream to achieve any significant contact time.

Although one significant industrial application has been stressed for the phenomena of absorption by charged droplets, it would be reasonable to extend this research to other forms of gas-liquid contact operations. Also, certain atmospheric phenomena, such as the presence of inexplicably large quantities of sulfates and nitrates in clouds and rainwater might be more fruitfully investigated in the light of surface charge.

CHAPTER II

THEORETICAL DEVELOPMENT

Groothuis and Kramers (12) have treated the case of absorption of sulfur dioxide by growing water droplets. Starting from the equation,

$$N'' = (c^* - c_o)\sqrt{\frac{D}{\pi\, t}} \qquad (1)$$

where:

N'' = rate of diffusion through the boundary per unit surface,

c^* = concentration at the boundary for $t>0$,

c_o = bulk concentration at $t = 0$,

D = diffusivity, and

t = time,

it has been shown that it is possible to make an estimate of the absorption of gas by a droplet being formed at the tip of a capillary subject to certain assumptions. These assumptions are:

1. Gas phase resistance is negligible.
2. Depth of penetration of the solute molecules is small compared with the radius of curvature of the surface.
3. As the drop grows, the new surface formed is fresh surface with concentration c_o.
4. The effects of turbulence within the drop may be ignored.

The results indicate that the absorption follows a semi-empirical rate equation of the form,

$$m(t) = KVt^{\frac{1}{2}} \tag{2}$$

where:

$m(t)$ = amount of SO_2 absorbed after time, t, moles

V = droplet volume at time, t, cm^3

K = mass transfer coefficient, for initial absorption

$$= \frac{4\ c_s}{3\sqrt{\pi}\ r_e}\ \sqrt{D}$$

c_s = surface concentration, moles/cm^3

D = diffusivity of SO_2 in aqueous phase, cm^2/sec

r_e = constant relating the volume of the droplet to its surface area at any time, dependent on the radius of the capillary.

The surface concentration, c_s, is normally determined for trace gases at equilibrium with the liquid phase by application of Henry's law. If some way could be found to increase this surface concentration then the absorption rate would also be increased. It is proposed that by applying electrical charge to the surface, the equilibrium surface concentration will increase, thereby enhancing the rate of absorption.

The surface region of the droplet will be considered as a monolayer of water molecules. Further, it will be assumed that the molecules are arranged according to the generally accepted view that the oxygen end of the water molecule dipole protrudes outward from the surface and the hydrogens point inward toward the bulk. This arrangement of the dipoles establishes an electrical double layer with other ions in solution. Potentials of between -0.1 and -0.2 volts have been measured at the air-water interface by Davies (8). The presence of this equilibrium surface

charge reduces the surface tension by opposing the "normal" surface attraction of the molecules. This effect can be considered to be a repulsive surface pressure, π_o, such that

$$\pi_o = \gamma_o' - \gamma_o \tag{3}$$

where a hypothetical surface tension, γ_o', is indicated to represent that surface tension present in the absence of any surface charge. The term γ_o represents the actual tensile stress at the air-water interface.

According to Adamson (1), this surface pressure may also be expressed by a two-dimensional equation of state, for dilute solutions:

$$\pi_o = \Gamma_o RT \tag{4}$$

where

Γ_o = surface area concentration of adsorbed solute molecules, moles/cm^2

R = gas constant

T = absolute temperature

Using a value for temperature of 300°K and the values of Loeb (17) of 10^{11} adsorbed ions/cm^2 of surface for the air-water interface, we obtain an estimated value for π_o of 4.14×10^{-3} dynes/cm^2 (See Appendix D).

The relation between the equilibrium surface pressure and an applied surface charge density, q, may be derived from Lippmann's extension of Gibb's adsorption theory:

$$\frac{\partial \pi_o}{\partial \phi} = - \frac{\partial \gamma}{\partial \phi} = q \tag{5}$$

$$\frac{\partial^2 \pi_o}{\partial \phi^2} = \frac{\partial^2 \gamma}{\partial \phi^2} = c \tag{6}$$

Integrating equation (6)

$$\pi_o^* = \pi_o + \frac{1}{2} c \phi^2 \tag{7}$$

and, since $\phi = \frac{q}{c}$

$$\pi_o^* = \pi_o + \frac{1}{2} \frac{q^2}{c} \tag{8}$$

where:

ϕ = applied voltage, statvolts

γ = surface tension, dynes/cm

c = capacitance of surface, statfarads/cm^2

q = surface charge density, statcoulombs

The asterisk denotes the applied charged state, while π_o is the ordinary surface pressure, resulting from the equilibrium surface potential.

The effect of the increased surface pressure on the molecular surface area should now be considered. The surface equation of state is

$$\Pi A = kT = \text{constant}$$

where the surface pressure Π allows only for kinetic movement in the surface film, which is restricted to take place in only two dimensions with kinetic energy $\frac{1}{2}$ kT in each. Therefore, at a constant temperature we may expect a decrease in the free area occupied by a moving surface molecule

as the surface pressure is increased. This effect resembles the reduction in volume occupied by a gas molecule as three dimensional pressure is increased in, say, a balloon.

With the area per molecule decreasing, the surface molecular density increases, yielding a greater number of water molecules per cm^2 of surface. Now, if a solute such as sulfur dioxide approaches a clean, uncharged air-water interface from the air, a fraction of the molecules will be adsorbed at the surface, hydrolyze, and pass into solution. Hydration of sulfur dioxide appears to be one of the most rapid hydrolytic reactions known and proceeds according to the following scheme (Schroetter) (22):

$$SO_2 + H_2O \underset{k_2}{\overset{k_1}{\rightleftharpoons}} HSO_3^- + H^+$$

where $k_1 = 3.4 \times 10^6 \text{ sec}^{-1}$

$k_2 = 2.0 \times 10^8 \text{ moles}^{-1} \text{ sec}^{-1}$

This hydration will take place directly upon adsorption.

The fraction of sulfur dioxide molecules that adsorb to the surface of the water must do so at a certain number of "sites." These sites are not fixed as in the case of solid catalysts, but will have a limited degree of two-dimensional movement and flexibility. In our research, we intended to increase the surface density of these sites by applying surface pressure by means of electrical charge. If n_o is the number of equilibrium surface sites available for sulfur dioxide adsorption, then, since

$$n^* A^* = n_o A_o$$

and $$\pi^* A^* = \pi_o A_o$$

we may write

$$\frac{n^*}{n_o} = \frac{\pi^*}{\pi_o} \tag{9}$$

Combining equations (8) and (9)

$$\frac{n^*}{n_o} = 1 + \frac{q^2}{2\pi_o c} \tag{10}$$

Assuming the surface concentration c_s is related to the number of sites in a linear relation,

$$\begin{aligned} c_s^* &= a\, n^* \\ c_s &= a\, n_o \end{aligned} \tag{11}$$

we may employ Henry's Law to determine this concentration:

$$c_s = H\, p_{SO_2}$$

where H is the Henry's Law constant and p_{SO_2} is the partial pressure of sulfur dioxide. In the charged condition, we may assume a similar relationship:

$$c_s^* = H^*\, p_{SO_2}$$

where the asterisk denotes the charged condition, and H* is a modified

Henry's Law constant.

Now by combining equations (9) and (11) we have,

$$c_s^* = c_s \left(\frac{\pi_o^*}{\pi_\sigma}\right) \tag{12}$$

and

$$c_s^* = c_s \left(1 + \frac{q^2}{2c\pi_\sigma}\right) \tag{13}$$

Returning to equation (2), it can be rewritten to account for the charged condition

$$m^*(t) = K^* V t^{\frac{1}{2}} \tag{14}$$

where K* is now defined by

$$K^* = \frac{4\, c_s^*}{3\sqrt{\pi}\, r_e} \sqrt{D} \tag{15}$$

and, substituting equation (11) gives

$$K^* = K\left(1 + \frac{q^2}{2c\pi_\sigma}\right) \tag{16}$$

Equation (16) forms the basis for this investigation. The Groothuis model originally assumed has been substantiated by Popovich (20) in an independent study. It is predicted by equation (16) that the mass transfer coefficient and, consequently, the rate of mass transfer increase according to the square of the surface electrical charge density.

CHAPTER III

INSTRUMENTATION AND EQUIPMENT

For the experiment an apparatus had to be constructed that could perform certain functions reliably and accurately. First, drops of water had to be generated and charged. Then these drops had to be contacted with a sulfur dioxide-air mixture in such a way that exposure would occur only during the drop formation period. Finally, the drops had to be collected and analyzed. Further, the apparatus was required to generate an air stream with humidity variable from dry to saturated conditions. Appropriate amounts of sulfur dioxide had to be metered into this stream to produce concentrations from 750-4000 parts per million in the gas phase. Measurements of the droplet size, its surface charge density, the concentration of the sulfur dioxide-air mixture, the droplet formation time, and the amount of sulfur dioxide absorbed were all required. Other pertinent parameters were: the water temperature, the sulfur dioxide-air mixture temperature, the relative humidity of the gas phases, the flow rates of all streams, and the applied voltage. Knowledge of these quantities allowed calculation of the rate of absorption, which could then be related to the surface charge density of the droplet. A schematic of the experimental apparatus and a drawing of the reactor vessel are included as Figures 1 and 2, respectively.

The separate components of the apparatus will be considered in groups according to their functions. The initial group was comprised of

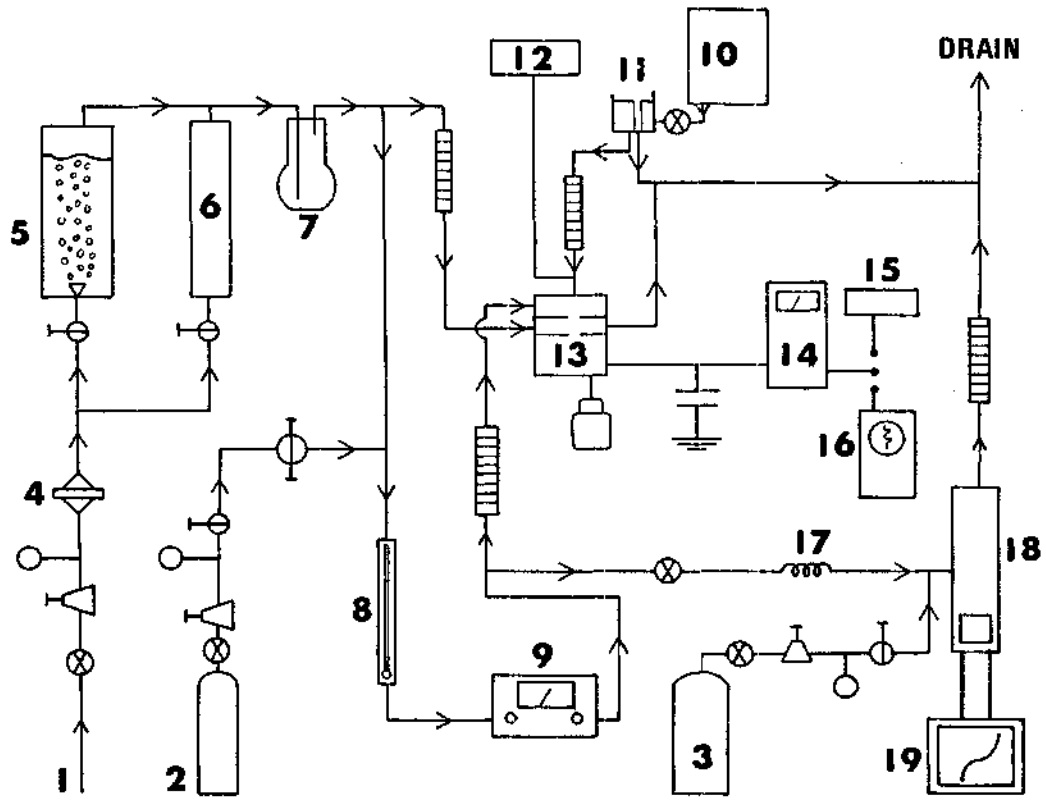

1. AIR SOURCE
2. DRY SO_2
3. DRY NITROGEN
4. MILLIPORE FILTER
5. HUMIDIFIER
6. DRYER
7. MIXING FLASK
8. THERMOMETER
9. DEW PT. HYGROMETER
10. H_2O RESERVOIR
11. CONSTANT HEAD PRESS. REG.
12. VOLTAGE SOURCE
13. REACTION CHAMBER
14. ELECTROMETER
15. DIGITAL VOLTMETER
16. OSCILLOSCOPE
17. COLD TRAP
18. SO_2 INFRARED ANALYZER
19. STRIP CHART

SYMBOLS

- VALVE
- PRESS. REG.
- PRESS. INDICATOR
- NEEDLE VALVE
- FINE METERING VALVE
- CAPACITOR
- ROTOMETER

Figure 1. Schematic Diagram of the Experimental Apparatus

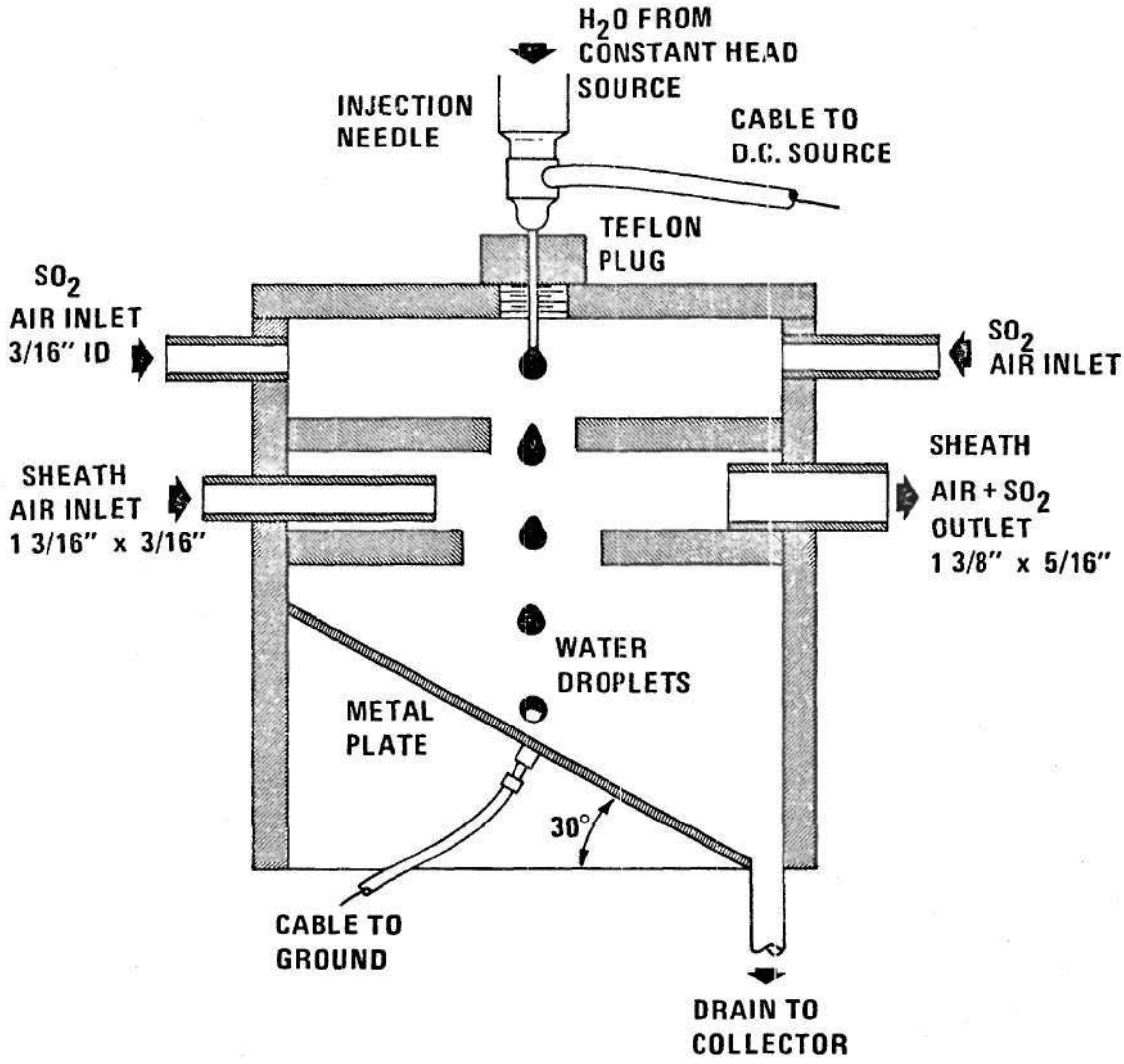

Figure 2. Sketch of the Reactor Vessel

those elements that produced the charged droplets. It consisted of a polyethylene reservoir, a constant-head water pressure regulator, a stopcock, a high voltage source, and a hypodermic needle. The water pressure regulator was a plexiglass cup which maintained a constant pressure head of water by means of a drain outlet at a fixed height. The entire device could be moved vertically to allow for selection of an appropriate water flow rate. Most of the water flowed into this device from the reservoir and then continued out the drain at the center. A small quantity of water, which flowed to the reaction chamber to become droplets, exited through an outlet in the bottom of the cup. The water used in the experiment was distilled, deionized water reduced to a total conductivity equivalent of less than 0.1 parts per million of sodium chloride. The water leaving the cup by the drain tube was discarded.

During the course of an experimental run, water flowed out of the reservoir, throught the pressure regulator, through a Matheson, Model 601, rotameter, through the stopcock, and through the needle to form the droplets. The needle was a no. 24 hypodermic which had been ground square and polished at the tip. The droplets were charged by means of a Beckman high voltage source variable from 0-25 kv which was electrically connected to the hypodermic needle. The voltage supply was stabilized and protected against unwanted current drain by the low pass filter of high resistance shown in Figure 3.

The next group consisted of those elements that produce and measure the gas streams. Included in the group was a metered supply of air of variable humidity, a metering system for the introduction of sulfur dioxide into the reactant gas stream, and EG & G, Model 880, dew point hygrom-

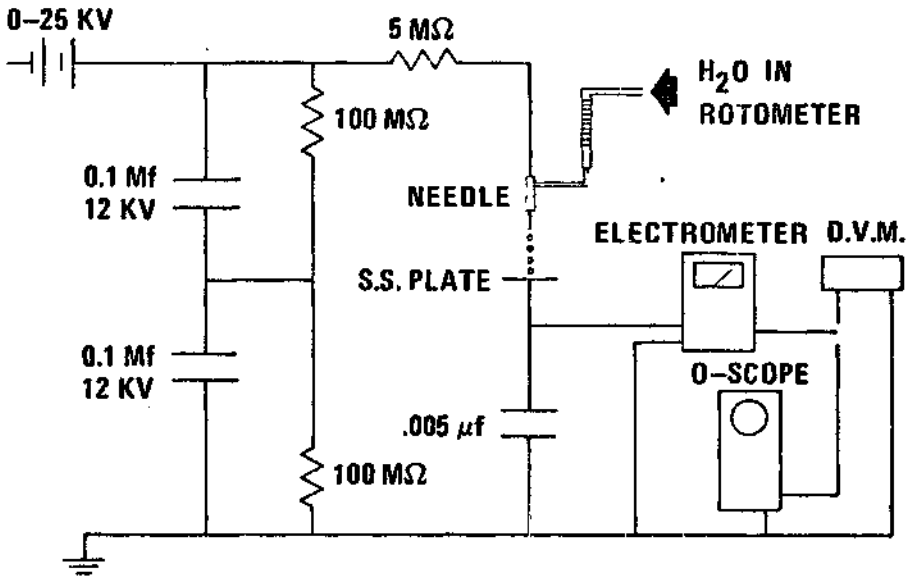

Figure 3. Diagram of the Electrical Apparatus

eter, a mercury thermometer, and a Bechman, Model 215A, nondispersive infrared analyzer. In the air supply, shop air was passed through a diaphragm type pressure regulator and then through a millipore filter. At this point the air was split into two streams. One stream was bubbled through a water column and the other passed through a column of silica gel for drying. The proportion of the inlet stream that passed through each column was controlled by needle valves on each of the two separate streams. This yielded a low humidity stream and a high humidity stream. At this point the streams were recombined for mixing. After mixing the stream was again divided into two streams. The first stream flowed through a Matheson, Model 604, rotameter and provided "flushing" air for the reaction chamber. The second stream was injected with sulfur dioxide to form the reactant gas stream. The metering system for the injection of sulfur dioxide consisted of a cylinder of anhydrous sulfur dioxide, a diaphragm type pressure regulator, a needle valve, and a Nupro fine metering valve.

The reactant gas stream then passed around a total immersion thermometer and into the dew point hygrometer. As the stream left the hygrometer, it was tapped for analysis by the infrared analyzer. This tap stream passed through a dry ice-acetone cold trap and into the analyzer which monitored the sulfur dioxide concentration. The cold trap was required to prevent the adverse effects of condensed moisture on the infrared analyzer. The flow rate through the analyzer was monitored by a Matheson, Model 73, rotameter. The remainder of the reactant stream continued through a Matheson, Model 603, rotameter to the reaction chamber where it contacted the charged droplets and then flowed to the drain.

The next group is the reaction chamber. It was a plexiglass cubicle 4 inches x 4 inches x 4 7/16 inches tall incorporating three compartments (see Figure 2). The top compartment was filled with the reactant gas stream and was where the absorption took place. The middle compartment was the flushing compartment. Flushing air entered this compartment through a fan-shaped nozzle and swept the reactant gas to the drain through the large drain opening located directly across the compartment from the flush air inlet nozzle. The lower compartment was the droplet-collecting compartment. The base plate was stainless steel fitted with an electrical connection to the outside and a short stainless steel liquid drain tube. All metal-to-plexiglass joints were sealed with RTV sealant. The hypodermic needle was mounted inside a Teflon plug, for electrical insulation, which screwed into the top of the chamber. The droplets fell from the needle through the concentric holes in the compartment dividers onto the stainless steel base plate and then ran out the liquid drain tube to a collection reservoir. The flushing air prevented any contact of sulfur dioxide with the water resting on the stainless steel plate. This did, however, introduce the problem of desorption, but this will be discussed later.

The next group consisted of those elements which measured the droplet parameters. The group included the previously mentioned Model 601 rotameter, a Condensor Products glass capacitor, a Keithley, Model 610C, electrometer, a Keithley, Model 6103A, voltage divider, a Hewlett-Packard, Model 120, oscilloscope, a Honeywell digital voltmeter, and a Standard timer. Two methods were used to measure the number of drops per unit of time. At low drop rates the time for fifty drops to fall was

measured with the timer. The drops were counted visually. At rapid drop rates, when this method was deemed inaccurate, the stainless steel plate at the bottom of the reactor was connected to the electrometer, which functioned as a high gain amplifier, and to the oscilloscope. As each droplet fell to the plate, a pulse was visible on the oscilloscope. In order for the pulse to be sharp, the reaction chamber was enclosed in grounded aluminum foil to block 60 cycle noise. To observe the charge delivered by the droplets, the plate was connected to the capacitor and the charge was stored. The voltage across the capacitor was monitored by the electrometer which, in turn, was monitored by the digital voltmeter. The RC time constant for the capacitive circuit is 3410 ± 25 seconds. The voltage divider was used in conjunction with the electrometer to measure the actual voltage applied to the needle. The divider served as a resistor chain across which the entire voltage was placed. The electrometer measured the voltage across 1/1000 of the resistance and thus measured only 1/1000 of the total applied voltage. The drop size was calculated from the water flow rate and the drop rate. From the drop rate and the charge delivered per unit of time, the charge per drop was calculated. These numbers were then combined to calculate the surface charge density.

The final group consisted of the elements used to collect and analyze the exposed droplets. The group was comprised of a stopcock, a volumetric flask, a pipette, reagent hydrogen peroxide, polyethylene sample bottles, an A.C. conductance meter, and a thermometer. Five milliliters of three percent hydrogen peroxide were pipetted into a sample bottle. When sufficient water had collected in the reservoir

below the reactant chamber, the stopcock was opened and twenty-five milliliters were delivered to the volumetric flask. This was then poured into the polyethylene sample bottle where the peroxide reacted with the sulfurous acid generated in the chamber to produce sulfuric acid and water. After samples from a number of runs were collected, the solutions were measured for temperature and conductance. The concentration could be determined from these two values.

This completes the description of the experimental apparatus. Details pertaining to the actual procedure of conducting a run are described in Chapter IV.

CHAPTER IV

PROCEDURE AND DATA ANALYSIS

The functions of this chapter are, first, to describe the procedure used in making an experimental run in sufficient detail to allow a technically competent person to go into the laboratory and conduct a typical run, and second, to analyzé the experimental data and make an estimate of the error involved in both the data and the calculations made using the data.

Prior to making an experimental run, certain preliminary actions were required. First, the electrometer, the oscilloscope, the strip chart recorder, and the dew point hygrometer were turned on for a minimum warm-up period of thirty minutes. The infrared analyzer, which would normally require a significant warm-up, was being kept in constant use by a group of graduate researchers and, therefore, was always maintained in the "ready" condition. While the other instruments were being warmed, the cold trap of dry ice and acetone was prepared, and the infrared analyzer was calibrated. To calibrate the analyzer, the zero gas, dry nitrogen, was passed through the instrument and the output was set to zero. Next, the span gas, a sulfur dioxide mixture of known concentration, was passed through the instrument and the gain was adjusted to obtain the reading that corresponded to the factory calibration curve for the known concentration. Then, the dry nitrogen line was again connected to the analyzer, and the zero point rechecked. The strip chart

recorder, which has a short warm-up time, was calibrated simultaneously with the infrared analyzer. After these checks, the gas and liquid streams were turned on and stabilized. Sulfur dioxide was added to the reactant gas stream until the concentration peculiar to the given run was attained. Also, the proportions of air passing through the humidifying column and the drying column were adjusted to select the humidity that was desired for the run. Since by this time all the instruments were sufficiently warmed-up, the dew point hygrometer could be used to monitor the humidity adjustment. The constant head water pressure regulator was adjusted to select an appropriate water flow rate. The high voltage source was turned on and the voltage applied to the needle was measured by means of the voltage divider and the electrometer. And finally, any water that had accumulated in the reactor during this setting-up period was drained and discarded.

At this point the run was in progress. Readings of the dew point hygrometer, the strip chart recorder, the dry bulb temperature of the gas streams, the temperature of the water, and the rotameters were made. These values were monitored throughout the run for constancy. Now the stainless steel plate was connected to the capacitor and the capacitor voltage gain was monitored by the electrometer. Readings were recorded at ten second intervals from zero to sixty seconds. Next, the drop rate was measured as indicated in Chapter III. The water flow rate was rechecked at the conclusion of these measurements. While waiting for sufficient solution to gather in the sample reservoir, five milliliters of three percent hydrogen peroxide were pipetted into a polyethylene sample bottle.

Now the sample which had been collecting in the reservoir was allowed to run rapidly into a twenty-five milliliter graduated cylinder. Twenty-five milliliters were withdrawn and added to the sample bottle with the hydrogen peroxide. The two solutions were mixed to allow the hydrogen peroxide to oxidize the sulfurous acid to sulfuric acid. This step was incorporated because sulfuric acid has a much lower vapor pressure than the dissolved sulfur dioxide.

The final step was the analysis of the sample. This was done conductometrically. The specific conductance of a sulfuric acid solution is a function only of its concentration and temperature (Willard, et al.) (24). The cell constant of the conductance meter was determined by preparing a 0.1 N solution of potassium chloride of known temperature. This solution was measured for conductance and, since the specific conductance of this solution is tabulated, the cell constant could be calculated. The cell constant was checked prior to each group of analyses. After verification of the cell constant, the sample solution was placed in a clean container and the conductance cell was lowered into it. The resistance and temperature were measured. From these values, the specific resistance of the sample solution could be calculated, and, by comparing this value with the calibration curve that was constructed for the cell, the concentration was determined.

This completes the description of an experimental run. In the majority of cases, two runs were made for each voltage-concentration-humidity combination. During the initial phase of the test program, tests were conducted in triplicate. Early results indicated that two trials would be sufficient. So, in the interest of time saving, the

duplicate procedure was adopted. This policy was further justified since it permitted data for an entire curve to be gathered in one day. This reduced the possibility that day-to-day changes, however slight, might have effect on a given curve.

Attention can now be turned to the second function of this chapter, the data analysis. Any errors were either reading errors or systematic errors. The latter type include those errors arising from instruments which were out of calibration or from using an instrument to measure a quantity for which it was not intended. In order to correct any erroneous instrument readings, the instruments were checked against more accurate standards. The infrared analyzer, the strip-chart recorder, and the conductance cell were calibrated before each use. The rotameters in the air flow were calibrated by measuring a volume of gas which passed at a constant rate by water displacement. It was found that the factory curves were accurate. The dew point hygrometer was found to read $0.5^{o}F$ low consistently. This assumed that the device was in balance. The balance was checked and adjusted, if necessary, every thirty minutes during experimentation. Comparison of flow rates of water measured by the Model 601 rotameter with the volume of water delivered in a given time showed that the factory curves for this rotameter were also accurate. The glass capacitor was measured by means of a Wheatstone bridge circuit and found to have a value of 4.88×10^{-9} farads at 1000 Hz. Observation of the discharge curve of this capacitor gave an RC time constant of 3410 ± 25 seconds. This implied a system electrical resistance of 6.98×10^{11} ohms, which was good isolation. The Keithley electrometer was calibrated against the fixed voltage stand-

ard furnished by Honeywell for the calibration of the digital voltmeter. It was found to be accurate. Comparison of the sweep time of the oscilloscope with a standard 60 Hz voltage source gave a correction factor of 1.011. The voltage divider was found to be accurate.

In each experiment, a number of assumptions were made about the validity of the measurements. For instance, it was assumed that the temperature of the gas streams was the same inside the reaction chamber as at the measuring points located in the upstream lines. The same assumption was made about the water line. Since the shop air temperature never differed from room temperature by more than 1.5°F, and, since the entire apparatus was in thermal equilibrium with the room air, little heat transfer should have occurred between reaction streams and the surroundings. Therefore, the assumptions seem justified.

Two of the most significant assumptions were that, first, no sulfur dioxide was absorbed by the water while it was collecting on the stainless steel plate, and, second, that no significant desorption occurred. To justify these assumptions, samples that already had been analyzed were placed in the bottom of the reaction chamber and allowed to remain there for a time equal to the normal duration of a run, viz., thirty minutes. Although the water flow was shut off, the gas streams were run in the usual manner. The sample was then re-analyzed. It was found that the resultant data point fell within the scatter already present in the data.

Due to the non-selectivity of the conductometric technique, it was necessary to establish a control value which could be used to adjust all experimental data points to determine the actual contribution of the

sulfur dioxide absorption. This was done by establishing a control curve for the case of zero parts per million sulfur dioxide in the reactant gas stream. The fact that such a condition existed was due to the presence of other species such as carbon dioxide in the reactant gas stream and the absorption of these species in addition to sulfur dioxide by the water droplets.

Next, the manner in which the data were used to calculate the quantities of interest will be reviewed. These quantities were:

1. the absorption coefficient, K, moles/cc-$sec^{\frac{1}{2}}$
2. the droplet volume, V, cc,
3. the droplet residence time, t, sec,
4. the number of moles absorbed per droplet, m(t), and
5. the surface charge density, q, statcoulombs/cm^2.

The surface charge density was calculated by

$$q = \frac{Q}{4(DR)\ \pi\ r^2} \tag{17}$$

where

Q = charge delivery rate, statcoulombs/min,

DR = drop rate, drops/min,

r = droplet radius, cm.

The charge delivery rate can be calculated from the capacitor charging curve

$$Q' = \frac{E_c}{R_s}\left[1 - \exp(-t_c/R_s C)\right]^{-1} \tag{18}$$

where

R_s = system resistance, ohms,

E_c = capacitor voltage at time t_c, volts,

t_c = time of voltage measurement, sec,

C = capacitance of the glass capacitor, farads,

Q' = charge delivery rate, coulombs/sec

and suitable conversions are made to units of minutes for time and to cgs electrostatic units of charge. The volume of each drop is calculated by dividing the volumetric flow rate of the water, F_w, by the drop rate, DR. From the volume of the drop, the radius of the drop was determined by use of

$$r = \sqrt[3]{\frac{3V}{4\pi}} \tag{19}$$

The number of moles per drop was calculated from

$$m(t) = MV\ (.001) \tag{20}$$

where M is the concentration of the sample solution in moles per liter taking into account the dilution by the peroxide. Finally, the absorption coefficient, K, was obtained from equation (2).

Having reviewed the calculations, the error produced by the inherent inaccuracies of the instruments or readings techniques was estimated. The quantity, q, is a function of DR, E_c, R_s, t_c, C, and F_w. The standard deviation in q, to a good approximation, is equal to the square root of the sum of the squares of the standard deviations of the parameters involved. These deviations are:

$d(c) = 0.2\%$ $\qquad$ $d(E_c) = 1\%$

$d(R_s) = 0.8\%$ $\qquad$ $d(t_c) = 1\%$

$$d(DR) = 0.3\% \qquad d(F_w) = 1.5\%$$

$$d(q) = 2.5\%$$

Similarly, K is a function of DR, F_w, T_r, R_c and the cell constant, θ. Since the variation in F_w and DR will cancel for the most part, the contribution of each of these items will be reduced by one-half, i.e.,

$$\tfrac{1}{2}\, d(F_w) = 0.75\% \qquad \tfrac{1}{2}\, d(DR) = 0.15\%$$

$$d(\theta) = 1\% \qquad d(R_c) = 2\%$$

$$d(T_r) = 1\%$$

$$d(K) = 2.6\%$$

This standard deviation correlates well with the average of the deviations, 2.5 percent, observed experimentally for K at zero charge density across all the humidities tested. The larger amount of scatter present in the data for the charged conditions could be the result of the higher fields present, but no predictions on this phenomena can be made based on this study alone.

CHAPTER V

DISCUSSION OF RESULTS

The experimentally measured parameters for all runs are listed in Appendix B. The calculated values for all runs are listed in Appendix C. Graphic presentation of these results are incorporated in this chapter.

Before describing the individual graphs, however, some general remarks about the data are in order. First, at the time of absorption, slight temperature changes occurred in the droplets due to the absorption. No effort was made to take these effects into account. Accurately quantifying such temperature changes was thought to be too difficult to do experimentally, and, also, it was thought that these effects would be inconsequential in comparison with other phenomena that were occurring. Second, flow rates were kept constant throughout the course of any given run, but there was slight run-to-run variation in the water flow rate through the capillary. Due to the small magnitude of this drift, which was of the order of 1% of the mean value, no special accounting of this change was attempted. Third, Schroetter (22) and other investigators have verified that the presence of surface agents may cause a reduction in the rate of sulfur dioxide absorption. Although distilled, de-ionized water was used exclusively in the experimentation, it was not known if any corrosion products had entered the water stream from the stainless steel hypodermic needle and stopcock. It should be remembered that this

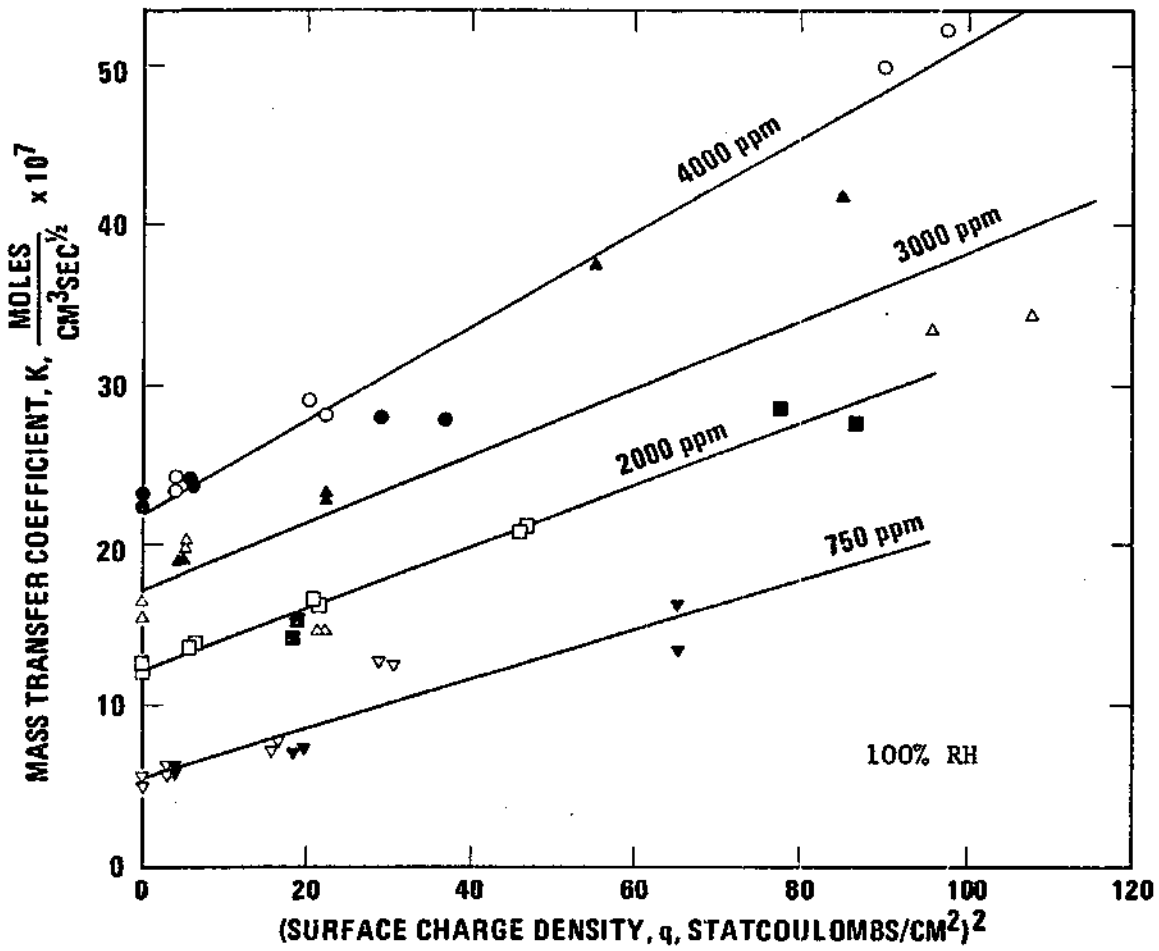

Figure 4. The Effect of Surface Charge Density on the Mass Transfer Coefficient, K, Observed for Four Gas-Phase Concentrations. (Shaded Symbols Indicate Positive Polarity; Open Symbols Indicate Negative Polarity.)

combination was being subjected to high voltage of both polarities throughout the trials. Such an error was assumed small, since both the stopcock and needle were cleaned prior to every series of runs. Finally, although charges of both polarities were applied to the droplets, no difference between the positive and negative situations was detected. With the above remarks in mind, description of the various curves can proceed.

The data analyzing the effect of solute concentration in the reactant gas stream on the absorption of sulfur dioxide by the charged droplets is shown as a family of lines in the graph of K vs. q^2 as may be seen in Figure 4. The linear variation of K with q^2 as predicted by equation (16) was verified experimentally. The actual lines represent a least squares fit of the data points. Further, the slopes of these lines change, increasing with concentration, also as predicted by equation (16).

In attempting to compare the values of K observed experimentally for the uncharged condition with those of Groothuis, it is found that this previous work obtained a value for the mass transfer coefficient, K, of 6.2×10^{-5} moles/cm^3-sec$^{\frac{1}{2}}$ while the present work produced values from $0.7 - 2.5 \times 10^{-6}$ in the same units. There are, however, a number of extenuating circumstances. Groothuis used a different size capillary, his time of exposure of the droplet ranged from one and one-half to fifty times as great as the longest droplet exposure time in these experiments, and his reactant stream was pure sulfur dioxide. The effect of the capillary variation, although uncertain, is certainly trivial. Addressing the second point, although the exposure time, t, appears in

the expression for K, the possibility of a change in mechanism exists as exposure times are lengthened. The effects of convection within the droplet, internal diffusion, and the relative validity of the "fresh surface" assumption all tend to play larger roles in the case of longer exposure times than in the case of the short exposure times present in this experiment. The third point will be discussed the following paragraphs.

The effect of reactant stream concentration is examined further in Figure 5, a plot of K vs. reactant stream concentration. A family of lines is presented to display the relationship at three values of surface charge density. If the line representing the uncharged state were extrapolated to a concentration of pure sulfur dioxide, the value of K would be, roughly, 50×10^{-5} in appropriate units. The magnitude of this extrapolation is quite large, but the only claim made, based on this value, is that the values for K obtained in this experiment are reasonably consistent with the assumed model of Groothuis.

The plots of K vs. q^2 provide another valuable piece of information. If the slope of each line is divided by its intercept, a value representing the quantity $\frac{1}{2}c\,\pi_o$ is obtained. The capacitance of the surface double layer, c, is related to the number of uncovered ions in the double layer and the voltage in the double layer by

$$c = \frac{Z\,e^-}{v}$$

where

Z = number of uncovered ions/cm^2

e^- = charge of an electron, statcoulombs

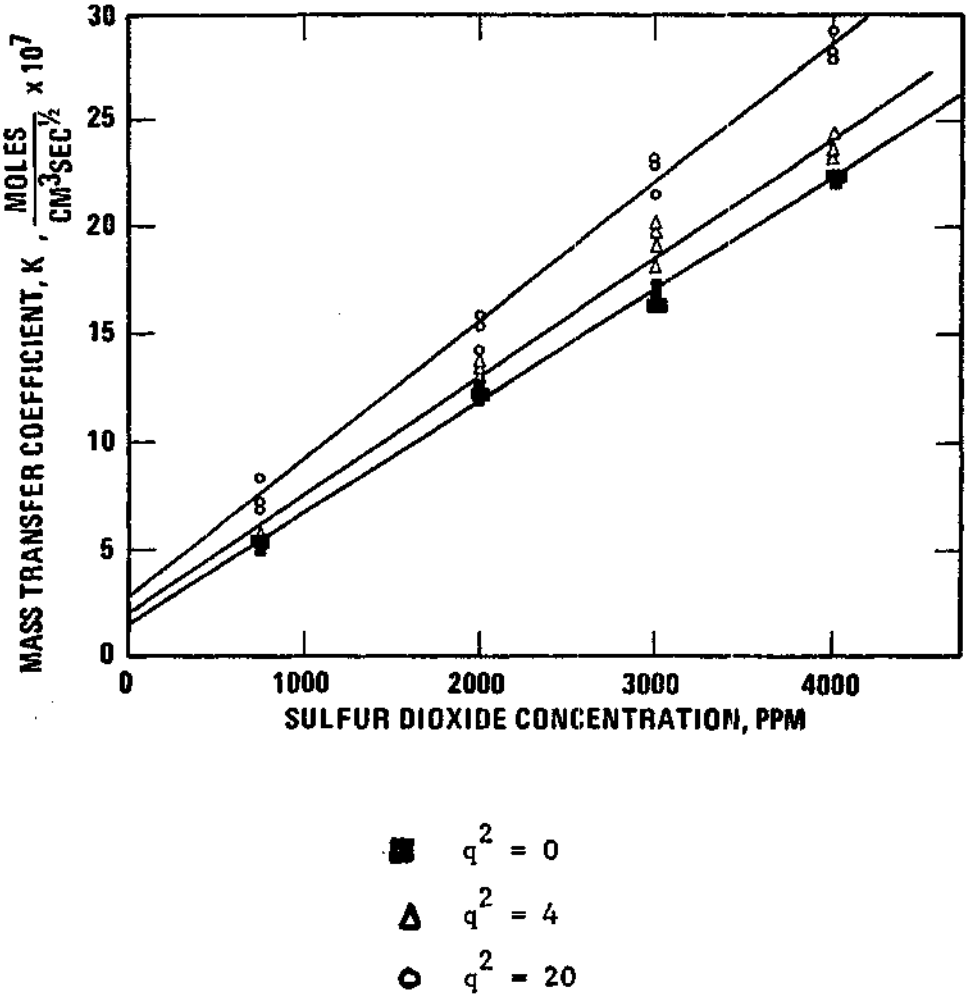

Figure 5. The Effect of Reactant Stream Concentration on the Mass Transfer Coefficient, K, of Charged Aqueous Droplets. (Three Values of q^2 Are Shown.)

v = voltage across the double layer, statvolts.

Taking the previously mentioned value of -0.1 volts as the value of v, the capacitance is then a constant times Z. The surface pressure, π_o, is calculated as indicated in Appendix D. At a given temperature, then, π_o is also a combination of constants times Z. Therefore, the quantity $\frac{1}{2}c\ \pi_o$ is really a combination of constants and the square of the number of uncovered ions in the double layer. By taking the average value of $\frac{1}{2}c\ \pi_o$ obtained from all of the plots of K vs. q^2 (see Appendix E), an experimental value of Z was calculated to be 2.5×10^{10} ions/cm^2. This value agrees closely with those obtained by other experimenters (Loeb) (17) of $10^9 < Z < 10^{11}$ ions/cm^2.

To represent the findings on the effect of relative humidity, Figures 6, 7, and 8 are presented. In Figures 6 and 7, the plots show K vs. q^2 at a constant reactant stream concentration of 2000 parts per million. Again, a family of lines is displayed. These lines describe the results at humidities of 0%, 35%, 50%, 70%, 90%, and 100%. The lines all have the characteristic slope-intercept feature, but no apparent order was present regarding the relative line-to-line position. To explore this further, a plot was made of K vs. percent relative humidity at two values of surface charge density. This plot is seen in Figure 8. The relative humidity is seen to have little effect on the value of K, regardless of charging condition.

The results obtained in this experiment tend to verify the absorption model of Groothuis. Also, the pronounced effect on absorption obtainable through surface charging of liquid droplets was demonstrated. Finally, the primary objective of this research, to examine the effects

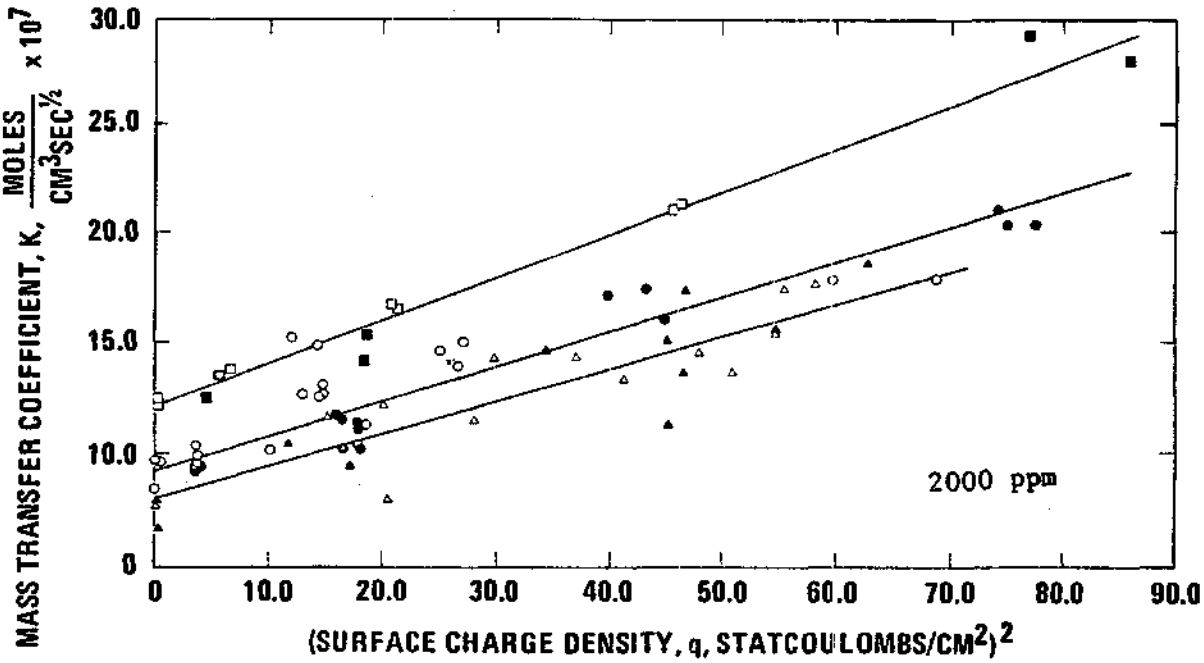

Figure 6. The Effect of Surface Charge Density on the Mass Transfer Coefficient, K, Observed for Three Values of Relative Humidity. (Shaded Symbols Indicate Positive Polarity; Open Symbols Indicate Negative Polarity.)

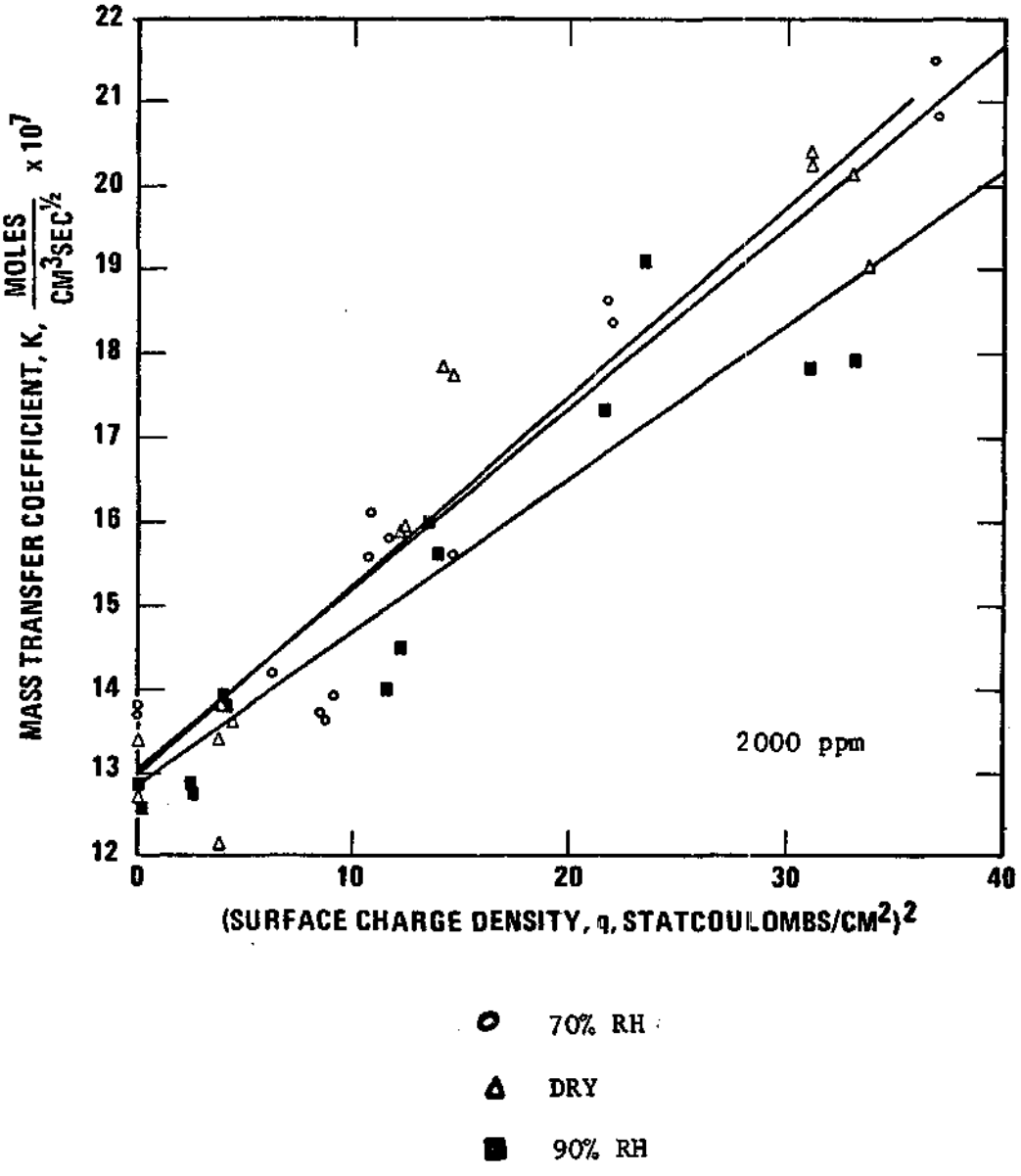

Figure 7. The Effect of Surface Charge Density on the Mass Transfer Coefficient, K, Observed for Three Values of Relative Humidity.

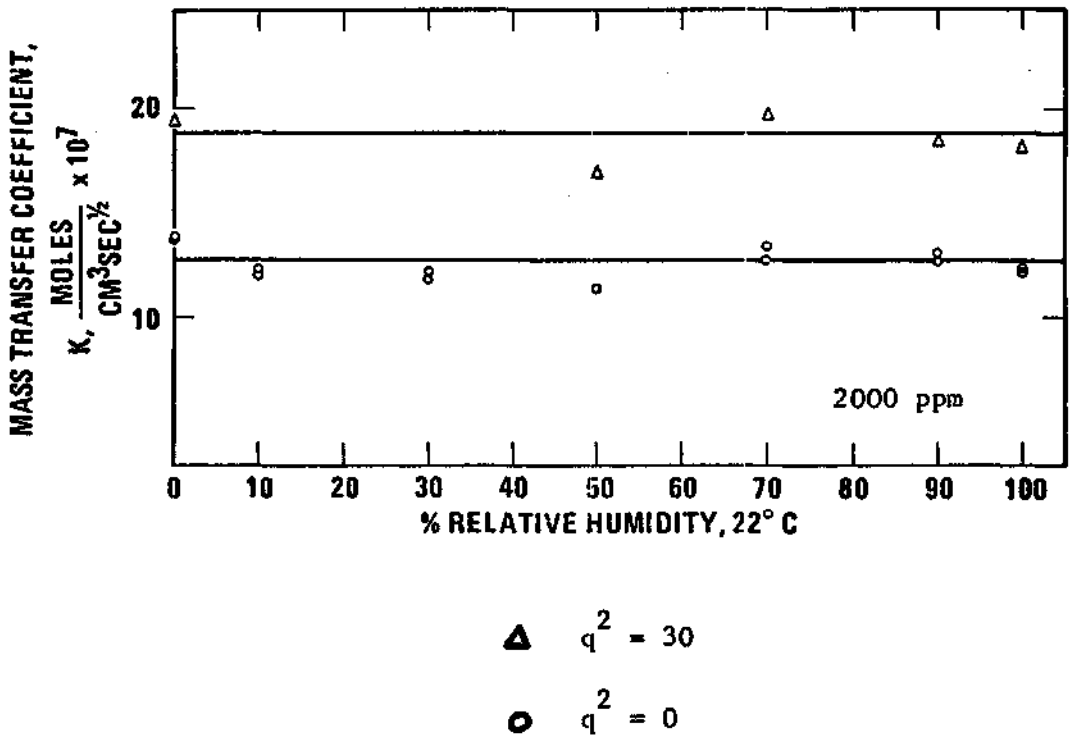

Figure 8. The Effect of Relative Humidity on the Mass Transfer Coefficient, K, of Charged Aqueous Droplets. (Two Values of q^2 Are Shown.)

of gas phase solute concentration and relative humidity on the absorption of sulfur dioxide by charged aqueous droplets, was satisfied.

The significance of this effort might be found in a number of areas. First, in industrial scrubbing the effectiveness of a spray tower scrubber, a spray venturi scrubber or any spray device might significantly be enhanced by applying electric surface charge to the droplet phase. The increased rate of absorption need not be limited to just sulfur dioxide or just scrubbing, either. Any type of gas-liquid operation where mass-transfer across a phase interface is occurring might be enhanced by this phenomena. Finally, as raindrops fall from the clouds, which already possess large quantities of ions, they may acquire additional charge due to static friction in passing through the atmosphere, and, as a result, absorb various ions from the air. This may account for the unusually high quantities of nitrates and sulfates in rainwater.

CHAPTER VI

CONCLUSIONS

In light of the preceeding results, the following conclusions may be drawn:

1. Changes in the relative humidity of the reactant gas stream have no measurable effect on the rate of sulfur dioxide absorption by either charged or uncharged droplets.

2. The absorption coefficient, K, and consequently, the rate of absorption of sulfur dioxide by water droplets increase with the square of the surface charge density of the droplets.

3. The absorption coefficient, K, and consequently, the rate of absorption, increase linearly with the concentration of sulfur dioxide in the reactant gas stream.

4. The "fresh surface" model of Groothuis as adapted for the charged condition of the droplets of this study affords a reliable means of predicting the increased rate of absorption of sulfur dioxide by cha charged aqueous droplets.

5. The value of 0.013 for the quantity $\frac{1}{2}c\ \pi_0$ is reasonable.

CHAPTER VII

RECOMMENDATIONS

From these results, it is expected that the use of electrical surface charge to enhance gas-liquid absorption rates could also be applied to other combinations besides just sulfur dioxide-water systems. Research into other combinations might yield results of value throughout industry. Also, little work has been done to determine the effects of capillary size. Selection of an optimum droplet source has yet to be determined. Work in this area is recommended.

APPENDIX A

NOMENCLATURE

Table 1. Nomenclature

a	Dummy constant
c	Capacitance of liquid droplet, statfarads
C	Capacitance of Glass Products capacitor, farads
c*	Surface concentration at gas-liquid boundary, moles/cm^3
c_o	Initial bulk concentration of solute in liquid phase, moles/cm^3
c_s	Surface monolayer concentration, moles/cm^3
c_s*	Surface monolayer concentration, charged condition, moles/cm^3
D	Diffusivity of SO_2 in water, cm^2/sec
DR	Drop rate, drops/min
e^-	Charge on an electron, statcoulombs
E_a	Applied voltage, volts
E_c	Capacitor voltage, volts
F_f	Volumetric flow rate of flushing air, cc/min
F_r	Volumetric flow rate of reactant gas, cc/min
F_w	Volumetric flow rate of water, cc/min
H	Henry's Law constant
H*	Modified Henry's Law constant
Hz	Cycles per sec
IR	Reading on infrared analyzer
k	Boltzman's constant
k_1	Reaction rate constant
k_2	Reaction rate constant
K	Mass transfer coefficient, moles/cc-$sec^{\frac{1}{2}}$

Table 1 (continued)

K^*	Mass transfer coefficient, charged condition, moles/cc-$sec^{\frac{1}{2}}$
$m(t)$	Moles of solute transferred, moles/drop
$m^*(t)$	Moles of solute transferred, charged condition, moles/drop
M	Adjusted concentration of sample solution, moles/liter
n_o	Number of equilibrium surface sites
n^*	Number of surface sites, charged condition
N''	Mass transfer rate, moles/cm^2
q	Surface charge density, statcoulombs/cm^2
Q	Charge delivery rate, statcoulombs/min
Q'	Charge delivery rate, coulombs/sec
r	Droplet radius, cm
r_e	Dimensional constant, cm
R	Gas constant
R_c	Sample resistance, ohms
R_s	System resistance, ohms
t	Droplet exposure time, sec
t_c	Time for voltage, E_c, to develop
T	Absolute temperature, ^oK
T_{db}	Dry bulb temperature, ^oF
T_r	Sample temperature, ^oC
T_{wb}	Wet bulb temperature, ^oF
v	Voltage across the double layer, statvolts
V	Droplet volume, cm^3
γ	Surface tension, dynes/cm^2

Table 1 (continued)

γ_o	Surface tension, charged condition, dynes/cm^2
γ_o'	Fictitious uncharged surface tension, dynes/cm^2
Γ_o	Surface concentration, moles/cm^2
ϕ	Voltage, volts
π	3.1415927...
π_o	Surface pressure, dynes/cm
π_o^*	Surface pressure, charged condition, dynes/cm
Π	Surface pressure, general
θ	Conductance cell constant
z	Number of uncovered ions/cm^2

APPENDIX B

EXPERIMENTALLY MEASURED VALUES

Table 2. Experimentally Measured Parameters

Run No.	DR	F_w	F_f	F_r	T_{db}	T_{wb}	IR	E_a	T_r	R_c
					2000 ppm - 50% RH					
1.	333.3	0.675	5420	1380	76	63	61.5	-5500	23.5	157
2.	333.3	0.675	5420	1380	76	63	61.5	-5500	23.5	160
3.	375.0	0.730	5380	1370	77	64	61.5	-5500	24.0	160
4.	300.0	0.730	5380	1370	77	64	61.5	-5500	24.0	149
5.	300.0	0730	5380	1370	77	64	61.5	-5500	24.0	149
6.	115.4	0.730	5380	1370	77	64	61.5	-4000	23.5	141
7.	115.4	0.730	5380	1370	77	64	61.5	-4000	23.5	140
8.	125.0	0.730	5380	1370	77	64	61.5	-4000	23.5	137
9.	214.0	0.730	5460	1380	75	63	61.5	-4000	23.5	160
10.	230.8	0.730	5460	1380	75	63	61.5	-4000	23.5	147
11.	240.0	0.730	5460	1380	75	63	61.5	-4000	23.5	147
12.	150.0	0.690	5460	1380	75	63	61.5	-3000	23.5	126
13.	150.0	0.690	5460	1380	75	63	61.5	-3000	23.5	120
14.	142.8	0.690	5460	1380	75	63	61.5	-3000	23.5	120
15.	106.2	0.680	5460	1380	75	63	61.5	-2000	23.5	117
16.	106.2	0.680	5460	1380	75	63	61.5	-2000	23.5	115
17.	105.3	0.680	5460	1380	75	63	61.5	-2000	23.5	113
18.	85.7	0.730	5460	1380	75	63	63.0	-1000	23.0	127

Table 2 (continued)

Run No.	DR	F_w	F_f	F_r	T_{db}	T_{wb}	IR	E_a	T_r	R_c
19.	83.3	0.710	5460	1380	75	63	63.0	-1000	23.0	123
20.	83.3	0.710	5460	1380	75	63	63.0	-1000	23.0	118
21.	60.9	0.650	5460	1360	74	63	62.0	0	23.0	118
22.	83.3	0.790	5460	1360	74	63	62.0	0	23.0	124
23.	82.2	0.790	5460	1360	74	63	62.0	0	23.0	125
24.	61.9	0.685	5460	1360	75	63	61.5	0	23.0	149
25.	61.9	0.685	5460	1360	75	63	61.5	0	23.0	135
26.	62.2	0.685	5460	1360	75	63	61.5	0	23.0	135
27.	89.6	0.780	5380	1360	75	63	61.5	+1000	24.0	136
28.	90.4	0.780	5380	1360	75	63	61.5	+1000	24.0	133
29.	90.4	0.780	5380	1360	75	63	61.5	+1000	24.0	133
30.	123.9	0.765	5380	1360	75	63	61.5	+2000	24.0	139
31.	123.9	0.765	5380	1360	75	63	61.5	+2000	24.0	147
32.	123.9	0.765	5380	1360	75	63	61.5	+2000	24.0	139
33.	120.5	0.785	5380	1360	75	63	61.5	+2000	24.0	144
34.	120.0	0.785	5380	1360	75	63	61.5	+2000	24.0	131
35.	121.5	0.785	5380	1360	75	63	61.5	+2000	24.0	132
36.	214.3	0.752	5380	1360	75	63	61.5	+3000	25.0	132
37.	200.0	0.740	5380	1360	75	63	61.5	+3000	25.0	134

Table 2 (continued)

Run No.	DR	F_w	F_f	F_r	T_{db}	T_{wb}	IR	E_a	T_r	R_c
38.	206.9	0.740	5380	1360	75	63	61.5	+3000	25.0	129
39.	300.0	0.685	5380	1360	75	63	61.0	+3500	25.0	135
40.	300.0	0.685	5380	1360	75	63	61.0	+3500	25.0	131
41.	300.0	0.696	5380	1360	75	63	61.5	+3500	25.0	135
					2000 ppm - 100% RH					
42.	600.0	0.710	5500	1370	76	76	61.5	+3080	21.5	137
43.	600.0	0.703	5500	1370	76	76	61.5	+3080	21.5	126
44.	111.5	0.710	5380	1370	75	75	61.5	+1910	21.5	138
45.	111.5	0.710	5380	1370	75	75	61.5	+1910	21.5	130
46.	82.2	0.685	5380	1370	73	73	61.5	+ 960	21.5	123
47.	82.2	0.710	5380	1370	73	73	61.5	+ 960	21.5	130
48.	63.6	0.685	5380	1380	73	73	61.5	0	21.5	118
49.	63.6	0.710	5380	1380	73	73	61.5	0	21.5	120
50.	80.6	0.650	5380	1380	75	74	61.5	- 885	22.8	95
51.	83.8	0.665	5380	1380	75	74	61.5	- 885	22.8	96
52.	116.3	0.665	5380	1380	75	74	61.5	-2020	22.8	97
53.	115.8	0.665	5380	1380	75	74	61.5	-2020	22.8	97
54.	187.5	0.675	5380	1380	77	77	61.5	-2600	22.8	99
55.	187.5	0.675	5380	1380	77	77	61.5	-2600	22.8	100

Table 2 (continued)

Run No.	DR	F_w	F_f	F_r	T_{db}	T_{wb}	IR	E_a	T_r	R_c
					3000 ppm - 100% RH					
56.	545.4	0.740	5380	1370	75	75	78	-3010	23.0	109
57.	400.0	0.740	5380	1370	75	75	78	-3010	23.0	96
58.	135.7	0.760	5380	1370	75	75	78	-2000	23.0	113
59.	132.2	0.740	5380	1370	75	75	78	-2000	23.0	112
60.	89.3	0.707	5340	1370	74	74	78	-1000	22.5	75
61.	89.3	0.707	5340	1370	74	74	78	-1000	22.5	73
62.	63.9	0.707	5340	1370	75	75	78	0	22.5	77
63.	63.9	0.707	5340	1370	74	74	78	0	22.5	73
64.	87.2	0.707	5340	1370	74	74	78	+1000	22.5	75
65.	87.7	0.707	5340	1370	73	73	78	+1000	22.5	76
66.	126.0	0.707	5340	1370	73	73	78	+2010	22.5	76
67.	123.4	0.707	5340	1370	74	74	78	+2010	22.5	76
68.	352.9	0.707	5340	1370	74	74	78	+2990	22.5	80
69.	375.0	0.700	5340	1370	74	74	78	+2990	22.5	77
					4000 ppm - 100% RH					
70.	250.0	0.705	5380	1350	75	75	90.5	+3000	21.5	67
71.	250.0	0.715	5380	1350	75	75	90.5	+3000	21.5	70
72.	125.5	0.715	5380	1350	75	75	90.5	+2030	21.5	68

Table 2 (continued)

Run No.	DR	F_w	F_f	F_r	T_{db}	T_{wb}	IR	E_a	T_r	R_c
73.	121.9	0.715	5380	1350	75	75	90.5	+2030	21.5	67
74.	82.2	0.715	5380	1350	75	75	90.5	+1010	21.5	63
75.	81.7	0.715	5380	1350	75	75	90.5	+1010	21.5	64
76.	81.9	0.758	5380	1375	70	70	90.5	0	21.5	66
77.	82.6	0.758	5380	1375	70	70	90.5	0	21.5	65
78.	88.8	0.753	5380	1375	70	70	90.5	- 990	21.5	65
79.	86.4	0.740	5380	1375	70	70	90.5	- 990	21.5	66
80.	114.1	0.705	5380	1375	70	70	90.5	-1990	21.5	65
81.	127.6	0.770	5380	1375	70	70	90.5	-1990	21.5	67
82.	428.8	0.775	5380	1375	70	70	90.5	-3000	21.5	70
83.	375.0	0.775	5380	1375	70	70	90.5	-3000	21.5	69
					750 ppm - 100% RH					
84.	333.3	0.753	5380	1375	72	72	31.0	-2950	22.0	155
85.	333.3	0.748	5380	1375	72	72	31.0	-2950	22.0	182
86.	122.9	0.748	5380	1375	72	72	31.0	-2000	22.0	175
87.	122.9	0.753	5380	1375	72	72	31.0	-2000	22.0	181
88.	88.8	0.748	5380	1375	72	72	31.0	-1040	22.0	175
89.	89.6	0.753	5380	1375	72	72	31.0	-1040	22.0	171
90.	79.0	0.740	5380	1375	72	72	31.0	0	22.0	173

Table 2 (continued)

Run No.	DR	F_w	F_f	F_r	T_{db}	T_{wb}	IR	E_a	T_r	R_c
91.	78.9	0.740	5380	1375	72	72	31.0	0	22.0	166
92.	86.8	0.740	5380	1375	72	72	31.0	+1010	22.0	166
93.	88.2	0.740	5380	1375	72	72	31.0	+1010	22.0	175
94.	120.5	0.740	5380	1375	72	72	31.0	+1930	22.0	170
95.	122.0	0.740	5380	1375	72	72	31.0	+1930	22.0	175
96.	333.3	0.740	5380	1375	72	72	31.0	+2960	22.0	191
97.	333.3	0.740	5380	1375	72	72	31.0	+2960	22.0	190
					2000 ppm - Dry					
98.	223.9	0.780	5380	1375	72	<10°	61.5	-2680	21.0	105
99.	225.6	0.775	5380	1375	72	<10°	61.5	-2680	21.0	104
100.	116.7	0.740	5380	1375	72	<10°	61.5	-1870	21.0	98
101.	124.0	0.780	5380	1375	72	<10°	61.5	-1870	21.0	99
102.	90.1	0.788	5380	1375	72	<10°	61.5	- 960	21.0	96
103.	90.0	0.788	5380	1375	72	<10°	61.5	- 960	21.0	94
104.	84.3	0.790	5380	1375	72	<10°	61.5	0	21.0	93
105.	84.9	0.788	5380	1375	72	<10°	61.5	0	21.0	92
106.	93.2	0.795	5380	1375	72	<10°	61.5	+ 960	21.0	96
107.	93.2	0.795	5380	1375	72	<10°	61.5	+ 960	21.0	97
108.	116.7	0.803	5380	1375	72	<10°	61.5	+1730	21.0	98

Table 2 (continued)

Run No.	DR	F_w	F_f	F_r	T_{db}	T_{wb}	IR	E_a	T_r	R_c
109.	116.7	0.795	5380	1375	72	<10°	61.5	+1730	21.0	98
110.	167.6	0.803	5380	1375	72	<10°	61.5	+2380	21.0	102
111.	167.6	0.803	5380	1375	72	<10°	61.5	+2380	21.0	100
					2000 ppm - 70% RH					
112.	178.6	0.780	5380	1375	72	65	61.5	+2400	23.0	106
113.	181.8	0.788	5380	1375	72	65	61.5	+2400	23.0	103
114.	115.8	0.788	5380	1375	72	65	61.5	+1540	23.0	100
115.	115.8	0.788	5380	1375	72	65	61.5	+1540	23.0	100
116.	85.7	0.788	5380	1375	72	65	61.5	+1010	21.5	105
117.	92.3	0.788	5380	1375	72	65	61.5	+1010	21.5	98
118.	83.6	0.790	5380	1375	72	65	61.5	0	21.5	98
119.	83.1	0.788	5380	1375	72	65	61.5	0	21.5	95
120.	91.7	0.788	5380	1375	72	65	61.5	-1020	21.5	99
121.	91.7	0.788	5380	1375	72	65	61.5	-1020	21.5	97
122.	116.3	0.788	5380	1375	72	65	61.5	-1800	21.5	98
123.	116.3	0.788	5380	1375	72	65	61.5	-1800	21.5	99
124.	190.5	0.788	5380	1375	72	65	61.5	-2510	21.5	102
125.	193.5	0.788	5380	1375	72	65	61.5	-2510	21.5	101

Table 2 (continued)

Run No.	DR	F_w	F_f	F_r	T_{db}	T_{wb}	IR	E_a	T_r	R_c
					2000 ppm - 90% RH					
126.	203.2	0.793	5380	1375	74	72	61.5	-2500	22.0	117
127.	189.9	0.765	5380	1375	74	72	61.5	-2500	22.0	112
128.	122.4	0.800	5380	1375	74	72	61.5	-1820	22.0	111
129.	121.6	0.793	5380	1375	74	72	61.5	-1820	22.0	108
130.	91.5	0.808	5380	1375	74	72	61.5	-1030	22.0	104
131.	91.2	0.808	5380	1375	74	72	61.5	-1030	22.0	102
132.	83.1	0.815	5380	1375	74	72	61.5	0	22.0	101
133.	82.4	0.808	5380	1375	74	72	61.5	0	22.0	101
134.	92.0	0.815	5380	1375	74	72	61.5	+1070	22.0	98
135.	92.2	0.815	5380	1375	74	72	61.5	+1070	22.0	98
136.	127.1	0.820	5380	1375	74	72	61.5	+1930	22.0	104
137.	128.8	0.820	5380	1375	74	72	61.5	+1930	22.0	103
138.	181.8	0.830	5380	1375	74	72	61.5	+2430	22.0	106
139.	179.6	0.845	5380	1375	74	72	61.5	+2430	22.0	112

APPENDIX C

CALCULATED VALUES

Table 3. Calculated Values

Run No.	r	V x 10^3	Q	t	m(t) x 10^9	q	q^2	M x 10^4	K x 10^7
				2000 ppm - 50% RH					
1.	0.0785	2.02	235.7	0.180	1.76	9.14	83.46	8.70	20.70
2.	0.0785	2.02	235.7	0.180	1.72	9.14	83.46	8.50	20.20
3.	0.0775	1.95	258.9	0.160	1.65	9.16	83.89	8.50	21.20
4.	0.0834	2.43	203.0	0.200	2.24	7.74	59.86	9.20	20.90
5.	0.0834	2.43	217.9	0.200	2.24	8.31	68.99	9.20	20.90
6.	0.1147	6.32	79.9	0.520	6.14	3.19	10.16	9.70	13.40
7.	0.1147	6.32	80.8	0.520	6.20	4.23	17.93	9.80	13.60
8.	0.1117	5.84	84.6	0.478	5.84	4.32	18.63	10.00	14.50
9.	0.0938	3.41	84.5	0.281	2.86	3.60	12.98	8.40	15.80
10.	0.0910	3.16	90.9	0.259	2.91	3.78	14.31	9.20	18.00
11.	0.0899	3.04	84.8	0.250	2.80	3.48	12.11	9.20	18.40
12.	0.1032	4.60	103.6	0.400	4.97	5.17	26.69	10.80	17.10
13.	0.1032	4.60	104.7	0.400	5.29	5.22	27.22	11.50	18.20
14.	0.1049	4.83	98.8	0.420	5.55	5.01	25.08	11.50	17.80
15.	0.1152	6.40	67.3	0.565	7.55	3.80	14.47	11.80	15.70
16.	0.1152	6.40	67.8	0.565	7.62	3.83	14.66	11.90	15.80
17.	0.1155	6.46	68.2	0.568	7.94	3.83	14.66	12.30	16.20
18.	0.1267	8.52	32.9	0.700	9.12	1.90	3.63	10.70	12.80

Table 3 (continued)

Run No.	r	V x 10^3	Q	t	m(t) x 10^9	q	q^2	M x 10^4	K x 10^7
19.	0.1267	8.52	32.6	0.720	9.46	1.94	3.77	11.10	13.10
20.	0.1267	8.52	31.9	0.720	9.80	1.90	3.61	11.50	13.60
21.	0.1365	10.66	0.0	0.985	12.26	0.00	0.00	11.50	11.60
22.	0.1307	9.36	0.0	0.720	10.30	0.00	0.00	11.00	12.90
23.	0.1313	9.49	0.0	0.720	10.25	0.00	0.00	10.80	12.90
24.	0.1382	11.07	0.0	0.970	9.96	0.00	0.00	9.00	9.12
25.	0.1382	11.07	0.0	0.970	11.07	0.00	0.00	10.00	10.15
26.	0.1380	11.01	0.0	0.963	11.01	0.00	0.00	10.00	10.20
27.	0.1276	8.71	34.6	0.688	8.88	1.89	3.56	10.20	12.40
28.	0.1272	8.63	34.9	0.665	8.98	1.90	3.60	10.40	12.70
29.	0.1272	8.63	36.5	0.665	8.98	1.98	3.94	10.40	12.70
30.	0.1138	6.17	85.3	0.483	6.11	4.23	17.90	9.90	14.25
31.	0.1138	6.17	85.9	0.483	5.74	4.26	18.14	9.30	13.40
32.	0.1138	6.17	85.1	0.483	6.29	4.22	17.82	10.20	14.60
33.	0.1158	6.51	82.0	0.500	6.18	4.04	16.30	9.50	13.40
34.	0.1160	6.54	80.2	0.500	6.87	3.95	15.60	10.50	14.90
35.	0.1155	6.46	82.2	0.500	6.72	4.04	16.30	10.40	14.70
36.	0.0943	3.51	158.7	0.279	3.76	6.30	39.69	10.70	20.30
37.	0.0959	3.70	155.1	0.300	3.88	6.70	44.96	10.50	19.20

Table 3 (continued)

Run No.	r	V x 10^3	Q	t	m(t) x 10^9	q	q^2	M x 10^4	K x 10^7
38.	0.0949	3.58	154.2	0.280	3.97	6.58	43.35	11.10	20.60
39.	0.0816	2.28	221.8	0.200	2.37	8.83	77.92	10.40	23.30
40.	0.0816	2.28	216.9	0.200	2.44	8.63	74.53	10.70	24.00
41.	0.0821	2.32	219.4	0.200	2.41	8.71	75.83	10.40	23.33
					2000 ppm - 100% RH				
42.	0.0656	1.18	263.6	0.100	1.13	8.12	66.00	9.55	30.7
43.	0.0654	1.17	283.1	0.100	1.17	8.78	77.18	10.40	31.9
44.	0.1150	6.37	79.2	0.540	5.99	4.28	18.28	9.45	17.3
45.	0.1150	6.37	79.8	0.540	6.37	4.31	18.54	10.00	18.5
46.	0.1258	8.33	34.4	0.730	8.99	2.11	4.43	10.80	12.6
47.	0.1273	8.64	34.0	0.730	8.64	2.03	4.12	10.00	11.7
48.	0.1370	10.77	00.0	0.940	12.16	0	0	11.20	11.6
49.	0.1388	11.21	00.0	0.940	12.08	0	0	11.00	11.1
50.	0.1244	8.06	37.3	0.743	11.68	2.38	5.67	14.50	16.8
51.	0.1237	7.94	40.6	0.715	11.43	2.52	6.35	14.40	17.0
52.	0.1109	5.72	82.2	0.515	8.15	4.57	20.90	14.25	19.9
53.	0.1111	5.74	83.0	0.518	8.18	4.62	21.34	14.25	19.8
54.	0.0951	3.60	145.1	0.319	4.97	6.81	46.39	13.80	24.5
55.	0.0951	3.60	144.1	0.319	4.95	6.76	45.74	13.75	24.3

Table 3 (continued)

Run No.	r	V x 10^3	Q	t	m(t) x 10^9	q	q^2	M x 10^4	K x 10^7
				3000 ppm - 100% RH					
56.	0.0687	1.38	336.4	0.110	1.70	10.41	108.31	12.50	37.4
57.	0.0762	1.85	285.9	0.150	2.64	9.81	96.16	14.25	36.9
58.	0.1102	5.60	95.3	0.443	6.66	4.60	21.19	11.90	17.9
59.	0.1102	5.60	91.8	0.452	6.72	4.55	20.70	12.00	17.9
60.	0.1237	7.92	36.9	0.670	14.86	2.15	4.61	18.75	22.9
61.	0.1237	7.92	36.9	0.673	15.25	2.15	4.61	19.25	23.5
62.	0.1382	11.06	00.0	0.938	19.91	0.00	0.00	18.00	18.6
63.	0.1382	11.06	00.0	0.938	21.29	0.00	0.00	19.25	19.8
64.	0.1246	8.11	36.9	0.690	15.21	2.17	4.70	18.75	22.3
65.	0.1244	8.07	36.4	0.683	14.72	2.14	4.57	18.25	22.1
66.	0.1103	5.62	91.4	0.476	10.25	4.74	22.49	18.25	26.5
67.	0.1110	5.73	90.0	0.485	10.46	4.71	22.20	18.25	26.1
68.	0.0878	2.83	254.7	0.170	4.89	7.45	55.50	17.25	42.0
69.	0.0764	1.87	254.3	0.160	3.36	9.24	85.46	18.00	45.0
				4000 ppm - 100% RH					
70.	0.0876	2.82	318.0	0.240	6.13	13.90	193.30	21.75	44.3
71.	0.0881	2.86	318.0	0.240	5.93	13.77	189.70	20.75	42.3
72.	0.1108	5.70	105.0	0.480	12.25	5.43	29.50	21.50	31.1
73.	0.1119	5.86	116.0	0.493	12.76	6.05	36.60	21.75	31.1

Table 3 (continued)

Run No.	r	V x 10^3	Q	t	m(t) x 10^9	q	q^2	M x 10^4	K x 10^7
74.	0.1276	8.70	40.1	0.730	20.35	2.38	5.67	23.40	27.4
75.	0.1278	8.75	41.4	0.732	20.13	2.46	6.05	23.00	26.9
76.	0.1302	9.25	00.0	0.733	20.35	0.00	0.00	22.00	25.7
77.	0.1298	9.17	00.0	0.725	20.64	0.00	0.00	22.50	26.5
78.	0.1265	8.47	37.0	0.676	19.07	2.07	4.28	22.50	27.4
79.	0.1269	8.56	35.6	0.695	19.06	2.03	4.11	22.25	26.7
80.	0.1138	6.18	88.5	0.523	14.06	4.75	22.60	22.75	31.4
81.	0.1129	6.03	91.9	0.469	13.28	4.48	20.10	22.00	32.1
82.	0.0755	1.81	304.5	0.140	3.75	9.86	97.30	20.75	55.4
83.	0.0790	2.07	280.0	0.160	4.39	9.49	90.00	21.25	53.0
84.	0.0814	2.26	223.2	0.180	1.87	8.04	64.61	8.30	19.5
85.	0.0812	2.24	223.4	0.180	1.59	8.09	65.51	7.10	16.7
86.	0.1132	6.08	87.5	0.487	4.50	4.42	19.55	7.40	10.6
87.	0.1135	6.12	85.4	0.487	4.41	4.29	18.41	7.20	10.3
88.	0.1262	8.42	37.0	0.676	6.23	2.08	4.33	7.40	9.0
89.	0.1261	8.40	35.4	0.668	6.39	1.98	3.92	7.60	9.3
90.	0.1307	9.36	00.0	0.757	7.04	0.00	0.00	7.52	8.6
91.	0.1308	9.37	00.0	0.761	7.24	0.00	0.00	7.72	8.8
92.	0.1267	8.52	34.6	0.692	6.31	1.97	3.89	7.40	8.9
93.	0.1260	8.39	34.0	0.681	6.47	1.94	3.77	7.72	9.4

Table 3 (continued)

Run No.	r	V x 10^3	Q	t	m(t) x 10^9	q	q^2	M x 10^4	K x 10^7
94.	0.1136	6.14	79.0	0.500	4.69	4.04	16.34	7.63	10.8
95.	0.1131	6.07	78.3	0.492	4.49	3.99	15.95	7.40	10.5
96.	0.0809	2.22	151.8	0.180	1.50	5.54	30.69	6.77	15.9
97.	0.0809	2.22	146.7	0.180	1.51	5.35	28.66	6.79	16.1
					2000 ppm - DRY				
98.	0.0940	3.48	151.2	0.269	4.35	6.08	36.94	12.50	24.0
99.	0.0936	3.43	156.7	0.267	4.38	6.31	39.80	12.75	24.8
100.	0.1148	6.34	73.9	0.515	8.53	3.82	14.61	13.45	18.8
101.	0.1145	6.29	66.1	0.484	8.43	3.28	10.48	13.40	19.3
102.	0.1278	8.74	53.9	0.666	12.02	2.92	8.50	13.75	16.9
103.	0.1274	8.66	46.2	0.670	12.30	2.49	6.22	14.20	17.4
104.	0.1308	9.38	00.0	0.713	13.36	0.00	0.00	14.25	16.9
105.	0.1303	9.27	00.0	0.706	13.25	0.00	0.00	14.30	17.0
106.	0.1268	8.53	56.9	0.644	11.73	3.02	9.13	13.75	17.2
107.	0.1268	8.53	55.6	0.644	11.52	2.95	8.73	13.50	16.8
108.	0.1180	6.88	66.8	0.515	9.25	3.27	10.69	13.45	18.8
109.	0.1176	6.81	69.3	0.515	9.16	3.42	11.67	13.45	19.0
110.	0.1046	4.79	107.9	0.358	6.18	4.68	21.95	12.90	21.6
111.	0.1046	4.79	107.6	0.358	6.27	4.67	21.80	13.10	21.8

Table 3 (continued)

Run No.	r	V x 10^3	Q	t	m(t) x 10^9	q	q^2	M x 10^4	K x 10^7
				2000 ppm - 70% RH					
112.	0.1014	4.37	113.9	0.336	5.63	5.80	33.70	12.90	22.9
113.	0.1011	4.33	130.3	0.330	5.80	5.58	31.16	13.40	23.4
114.	0.1175	6.80	70.6	0.518	9.35	3.52	12.35	13.75	19.1
115.	0.1175	6.80	70.2	0.518	9.35	3.49	12.20	13.75	19.1
116.	0.1299	9.19	35.7	0.700	11.71	1.96	3.85	12.75	15.3
117.	0.1268	8.53	39.1	0.650	11.52	2.10	4.39	13.50	16.8
118.	0.1312	9.45	00.0	0.718	12.76	0.00	0.00	13.50	15.9
119.	0.1313	9.48	00.0	0.721	13.46	0.00	0.00	14.20	16.6
120.	0.1270	8.58	35.8	0.654	11.54	1.92	3.70	13.45	16.6
121.	0.1270	8.58	36.4	0.654	11.80	1.96	3.84	13.75	17.0
122.	0.1174	6.77	75.7	0.515	9.14	3.76	14.11	13.50	21.0
123.	0.1174	6.77	76.4	0.515	9.11	3.79	14.39	13.45	20.9
124.	0.0996	4.13	138.5	0.315	5.40	5.83	34.03	13.05	23.3
125.	0.0990	4.07	133.2	0.310	5.33	5.59	31.22	13.10	23.6
				2000 ppm - 90% RH					
126.	0.0976	3.90	135.8	0.295	4.45	5.58	31.12	11.40	21.0
127.	0.0987	4.03	133.6	0.316	4.75	5.75	33.04	11.80	21.1
128.	0.1160	6.54	70.6	0.490	7.84	3.41	11.64	12.00	17.2

Table 3 (continued)

Run No.	r	V x 10^3	Q	t	m(t) x 10^9	q	q^2	M x 10^4	K x 10^7
129.	0.1159	6.52	71.5	0.494	8.08	3.48	12.13	12.40	17.7
130.	0.1282	8.83	30.1	0.656	11.39	1.60	2.54	12.90	16.0
131.	0.1283	8.86	29.4	0.658	11.60	1.56	2.44	13.10	16.2
132.	0.1328	9.81	00.0	0.722	13.14	0.00	0.00	13.40	15.8
133.	0.1327	9.80	00.0	0.729	13.47	0.00	0.00	13.75	16.1
134.	0.1284	8.86	37.8	0.652	12.18	1.98	3.92	13.75	17.0
135.	0.1283	8.84	36.7	0.651	12.16	1.93	3.71	13.75	17.1
136.	0.1155	6.45	79.5	0.472	8.32	3.73	13.92	12.90	18.8
137.	0.1150	6.37	78.4	0.466	8.31	3.66	13.42	13.05	19.2
138.	0.1029	4.56	117.1	0.330	5.82	4.84	23.45	12.75	22.3
139.	0.1040	4.70	113.6	0.334	5.55	4.65	21.66	11.80	20.5

APPENDIX D

CALCULATION OF π_o

$$\pi_o = \Gamma_o RT$$

if $R = 8.3 \times 10^7$ ergs/^oK-mole

$T = 300\ ^oK$

and $$\Gamma_o = \frac{10^{11}\ \text{ions/cm}^2}{6.023 \times 10^{23}\ \text{ions/mole}} = .166 \times 10^{-12}\ \text{moles/cm}^2$$

then

$$\pi_o = (.166)\ (10^{-12})\ (300)\ 8.3\ (10^7)$$

$$\pi_o = 2490\ (.166)\ 10^{-5}$$

$$\pi_o = 4.14 \times 10^{-3}\ \text{ergs/cm}^2$$

APPENDIX E

CALCULATION OF THE NUMBER OF UNCOVERED IONS IN THE SURFACE DOUBLE-LAYER

Table 3. Values of the Quantity $\frac{1}{2}c\,\pi_o$

Reactant Stream Concentration, ppm	Relative Humidity, %	$\frac{1}{2}c\,\pi_o$
2000	0	.0133
2000	35	.0134
2000	50	.0127
2000	70	.0137
2000	90	.0115
2000	100	.0126
750	100	.0179
3000	100	.0103
4000	100	.0120
	AVG:	.0130

Calculation of Z

$$\frac{1}{2c\,\pi_o} = .0130$$

$$c\,\pi_o = 38.35$$

$$Z^2 = \frac{38.35\ (6.023 \times 10^{23})}{(4.8 \times 10^{-10})\ 300(8.3 \times 10^{7})300}$$

$$Z^2 = 6.44 \times 10^{20}$$

$$Z = 2.54 \times 10^{10}\ \text{ions/cm}^2$$

BIBLIOGRAPHY

1. A. W. Adamson, Physical Chemistry of Surfaces, Second Edition, Interscience Publishers, New York, New York (1967) p. 95.

2. J. B. Angelo, E. N. Lightfoot, and D. H. Howard, "Generalization of the Penetration Theory for Surface Stretch: Application to Forming and Oscillating Drops," A.I.Ch.E. Journal, 12, 4, 751 (1966).

3. Y. Beers, Theory of Error, Addison-Wesley Publishing Company, Cambridge, Massachusetts (1953) p. 34.

4. J. J. Bikerman, Surface Chemistry, Second Edition, Academic Press, New York, New York (1958).

5. R. B. Bird, W. E. Stewart, and E. N. Lightfoot, Transport Phenomena, Wiley Publishing Company, New York, New York (1960) p. 656.

6. J. M. Coulson and S. J. Skinner, "The Mechanism of Liquid-Liquid Extraction Across Stationery and Moving Interfaces," Chemical Engineering Science, 1, 5, 197 (1952).

7. P. V. Danckwerts, "Significance of Liquid-Film Coefficients in Gas Absorption," Industrial and Engineering Chemistry, 43, 6, 1460 (1951).

8. J. T. Davies and E. K. Rideal, Interfacial Phenomena, Academic Press, New York, New York (1963).

9. J. L. Davis, "Absorption of Sulfur Dioxide by Charged Aqueous Droplets," Masters Thesis in Physics, Georgia Institute of Technology, 1972.

10. B. E. Dixon and A. A. Russel, "The Absorption of Carbon Dioxide by Liquid Drops," Journal of the Society of the Chemical Industry, 69, 284 (1950).

11. F. H. Garner, A. Foord, and M. Tayeban, "Mass Transfer From Circulating Liquid Drops," Journal of Applied Chemistry, 9, 315 (1959).

12. H. Groothuis and H. Kramers, "Gas Absorption by Single Drops During Formation," Chemical Engineering Science, 4, 17 (1955).

13. R. Higbie, "The Rate of Absorption of a Pure Gas Into a Still Liquid During Short Periods of Exposure," Trans. A.I.Ch.E., 31, 365 (1935).

14. H. F. Johnstone and P. W. Leppla, "The Solubility of Sulfur Dioxide at Low Partial Pressure," Journal of the American Chemical Society, 56, 2233 (1934).

15. W. Licht and J. B. Conway, "Mechanism of Solute Transfer in Spray Towers," Industrial and Engineering Chemistry, 42, 6, 1151 (1950).

16. W. Licht and W. F. Pansing, "Solute Transfer from Single Drops in Liquid-Liquid Extraction," Industrial and Engineering Chemistry, 45, 9, 1885 (1953).

17. L. B. Loeb, Static Electrification, Springer-Verlag Publishing, Berlin, Germany (1958) p. 86.

18. A. M. Marks, "Charged Aerosols for Air Purification and Other Uses," a paper presented to the 1971 National Meeting of the American Institute of Chemical Engineers.

19. J. H. Perry, Chemical Engineers Handbook, Fourth Edition, McGraw-Hill Book Company, New York, New York (1963).

20. A. T. Popovich, R. E. Jervis, and O. Trass, "Mass Transfer During Single Drop Formation," Chemical Engineering Science, 19, 357 (1964).

21. S. M. Rajan and W. J. Heideger, "Drop Formation Mass Transfer," A.I.Ch.E. Journal, 17, 1, 202 (1971).

22. L. C. Schroetter, Sulfur Dioxide, Pergamon Press Inc., New York, New York (1966).

23. T. K. Sherwood, J. E. Evans, and J. V. A. Longcor, "Extraction in Spray and Packed Columns," Trans. A.I.Ch.E., 35, 363 (1926).

24. H. H. Willard, L. L. Merritt, and J. A. Dean, Instrumental Methods of Analysis, Fourth Edition, Van Nostrand Company, Inc., Princeton, New Jersey (1965).